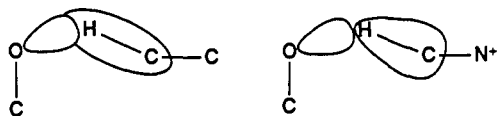


reactant-like. A similar effect could occur here. We suggest that the decrease in activation entropy reflects a decreased probability that the electron-deficient oxygen atom will encounter electron density on the hydrogen atom in OTMABP at the molecular geometry corresponding to the TS for OTBBP. In order to achieve comparable overlap, the methyl group of OTMABP must move closer to the oxygen, with an expected decrease in entropy and increase in enthalpy. In such a sterically crowded system there are two possible explanations for the two molecules having the same ΔH^\ddagger : either their TSs have essentially the same geometry and ΔS^\ddagger reflects electron density, or the enthalpy increase caused by extra motion of a methyl toward oxygen in OTMABP is offset by relief of nonbonded interactions elsewhere.



We are unaware of other studies that separate the inductive effects on rate constants of radical-like hydrogen transfer into enthalpy and entropy contributions. Consequently we are studying other, similar systems in order to establish how general this phenomenon of entropy control may be. In this regard it is noteworthy that 24tBBP is less reactive than OTBBP, showing the expected small inductive deactivation by a *p*-alkyl group,¹³ and the difference is almost entirely in their entropies of activation.

Acknowledgment. This work was supported with the help of NSF Grant No. CHE-88-05502. We thank Dr. Tito Scaiano of Ottawa University, until recently at the National Research Council of Canada, for his enthusiastic cooperation in making his flash kinetics apparatus available.

Registry No. OTMABP·BF₃, 136579-87-8; OTBBP, 22679-53-4; 2,4-*t*-BBP, 111959-99-0; D₂, 7782-39-0.

(13) Wagner, P. J.; Truman, R. J.; Scaiano, J. C. *J. Am. Chem. Soc.* **1985**, *107*, 7093.

Characterization of Complexes between Esters and Lithium Hexamethyldisilazide

Paul G. Williard* and Qi-Yong Liu

Department of Chemistry, Brown University
Providence, Rhode Island 02912

Lubomír Lochmann

Institute of Macromolecular Chemistry
Czechoslovak Academy of Sciences
162 06 Prague 6, Czechoslovakia

Received January 16, 1991

Proton transfer, i.e., enolization, proceeds readily under preparatively useful conditions upon reaction of lithium hexamethyldisilazide (LiHMDS) (1) with most ketone substrates. It has been noted by Heathcock et al. that LiHMDS fails to react with enolizable ester and amide substrates under the same conditions, i.e., THF solution at $\sim -78^\circ\text{C}$.¹ Yet there exist a few examples in which LiHMDS has been utilized to enolize esters.²

(1) Heathcock, C. H.; Buse, C. T.; Kleschich, W. A.; Pirrung, M. C.; Sohn, J. E.; Lampe, J. *J. Org. Chem.* **1980**, *45*, 1066.

(2) (a) Gamboni, R.; Tamm, C. *Helv. Chim. Acta* **1986**, *69*, 615. (b) Gennari, C.; Bernardi, A.; Colombo, L.; Scolastico, C. *J. Am. Chem. Soc.* **1985**, *107*(20), 5812. (c) Ireland, R. E.; Daub, J. P. *J. Org. Chem.* **1981**, *46*, 479.

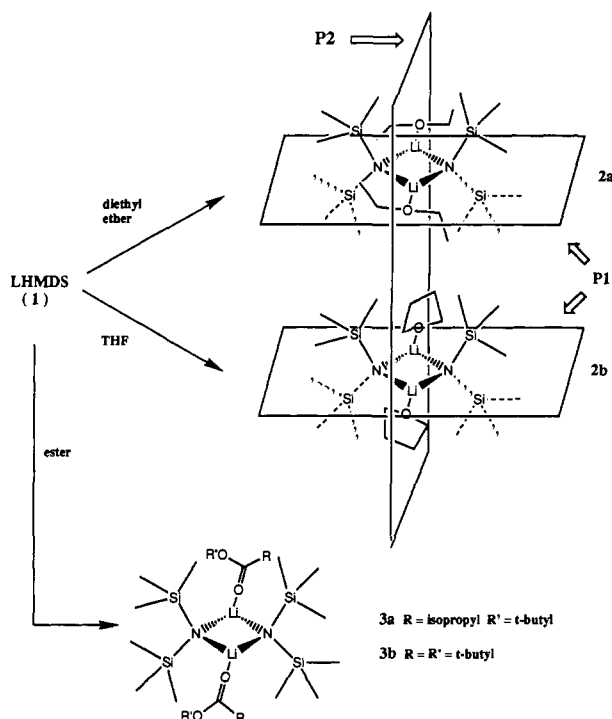


Figure 1. Coordination geometry of the LiHMDS dimer solvated with diethyl ether (2a) and with tetrahydrofuran (2b) (from their crystal structures) and expected geometry of the ester complexes (3).

While we do not propose to offer the explanation for these contradictory reports of the kinetic competence of LiHMDS to enolize esters, we now present evidence for the existence of stable complexes between LiHMDS and ester substrates both in solution and in the solid state.³

Evidence for an intermediate adduct between sodium hexamethyldisilazide (NaHMDS) and carboxylic esters in solution was previously reported by one of us.⁴ This adduct was characterized by a carbonyl absorption in the IR spectrum that is lowered relative to free ester by about 20–40 cm^{-1} due to coordination with an organometallic compound.⁵ The intensity of the coordinated ester carbonyl band was shown to decrease with time proportional to the intensity increase of both the ester enolate band (at 1665 cm^{-1}) and the HMDS free amine band (at 3370 cm^{-1}). We now have similar IR evidence that adducts are formed between LiHMDS and the three esters *tert*-butyl pivalate, methyl pivalate, and *tert*-butyl isobutyrate in benzene solution. An adduct is not completely formed between LiHMDS and *tert*-butyl pivalate since both free ester (1723 cm^{-1} , strong, roughly 40%) and coordinated ester (1686 cm^{-1} , strong, roughly 60%) bands are observed. Analogous bands (1732 cm^{-1} , weak inflex, and 1702 cm^{-1} , very strong) appear in the methyl pivalate spectrum. The IR spectrum of the LiHMDS/*tert*-butyl isobutyrate mixture shows only two relevant bands (1728 cm^{-1} , weak, and 1685 cm^{-1} , very strong). The upper band is attributed to free ester, and the lower band in this latter spectrum is close to that of the pure lithium enolate (1671 cm^{-1} in Nujol). Only a relatively weak HMDS absorption corresponding to a maximum of roughly 25% enoli-

(3) For recent discussions of aggregates of a variety of lithium amide bases in solution, see: (a) Galiano-Roth, A. S.; Kim, Y.-J.; Gilchrist, J. H.; Harrison, A. T.; Fuller, D. J. *J. Am. Chem. Soc.* **1991**, *113*, 5053. (b) Hall, P.; Gilchrist, J. H.; Collum, D. B. *J. Am. Chem. Soc.*, manuscript in press. (c) Hall, P.; Gilchrist, J. H.; Harrison, A. T.; Fuller, D. J.; Collum, D. B. *J. Am. Chem. Soc.*, manuscript in press. (d) Romesberg, F. E.; Gilchrist, J. H.; Harrison, A. T.; Fuller, D. J.; Collum, D. B. *J. Am. Chem. Soc.* **1991**, *113*, 5751. (e) Gilchrist, J. H.; Collum, D. B. *J. Am. Chem. Soc.*, manuscript in press.

(4) Lochmann, L.; Trekoval, J. *J. Organomet. Chem.* **1975**, *99*, 329.

(5) (a) Pasynkiewicz, S.; Starowieyski, K. *Roczniki Chem.* **1967**, *41*, 1139. (b) Lappert, M. F. *J. Chem. Soc.* **1961**, 817; **1962**, 542; **1965**, 5826. (c) Lochmann, L.; Sorm, M. *Collect. Czech. Chem. Commun.* **1973**, *38*, 3449.

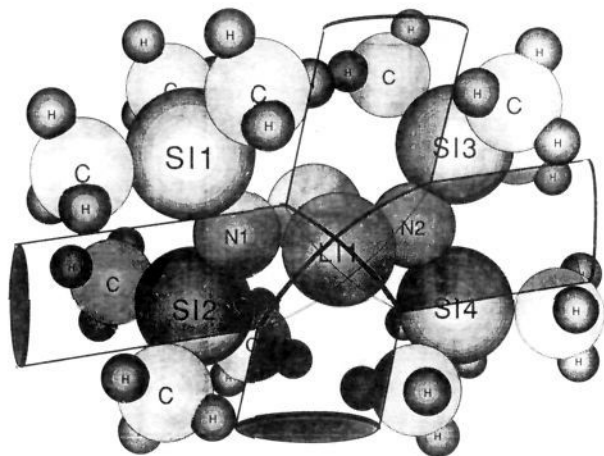


Figure 2. Computer-generated plot of the LiHMDS dimer from the crystal structures with ligands absent but emphasizing ligand-accessible space outlined by the superimposed cylinders. The intranuclear distances $\text{Si}(1)\text{--}\text{Si}(2) = 2.985 \text{ \AA}$ and $\text{Si}(1)\text{--}\text{Si}(3) = 4.876 \text{ \AA}$ suggest that approach of a ligand is slightly less sterically hindered in the vertical direction than in the horizontal direction although this is not the geometry that is found in any of the bis-solvated LiHMDS dimers, i.e., structures **2a,b** and **3a,b**.

zation is observed within the first 2 h at room temperature.

Although LiHMDS forms an uncharacteristic solid, cyclic trimer in the absence of heteroatom donors, it was shown to exist as a bis-solvated dimer, **2a** or **2b**, with diethyl ether or THF, respectively.⁶ An important reference plane associated with the ether ligands in **2a** and **2b** is the plane containing the ether oxygen and its two attached carbon atoms. This plane is nearly identical to but not exactly coplanar with the horizontal symmetry planes (P1) depicted in Figure 1 containing the Li–N–Li–N core of the dimers.⁷ Dihedral angles between the ether reference planes defined above and P1 are $\sim 5^\circ$ in **2a** and $\sim 23^\circ$ in **2b**.⁸

Another important reference plane depicted in Figure 1 is the vertical plane (P2), which also bisects the LiHMDS dimer. Either the horizontal plane (P1) or the vertical plane (P2) is sterically accessible for approach of a heteroatom donor. This point is illustrated in Figure 2 as a space-filling plot of an empty face of the LiHMDS dimer onto which we superimposed two estimated substrate-accessible cylinders.⁹ Analysis of Figure 2 reveals very little steric bias in favor of binding to the LiHMDS dimer from either the horizontal or the vertical direction. Hence the preference for coordination from the P1 plane in both **2a** and **2b** must be dominated by stereoelectronic factors rather than steric factors alone.¹⁰

We now report the results of two new X-ray crystal structures of the bis-solvated LiHMDS dimers **3a** and **3b** coordinated to *tert*-butyl isobutyrate and *tert*-butyl pivalate, respectively.¹¹

(6) (a) Lappert, M.; Slade, M.; Singh, A.; Atwood, J.; Rogers, R.; Shakir, R. *J. Am. Chem. Soc.* **1983**, *105*, 302. (b) Engelhardt, L. M.; May, A. S.; Raston, C. L.; White, A. H. *J. Chem. Soc., Dalton Trans.* **1983**, 1671. (c) Engelhardt, L. M.; Jolly, B. S.; Junk, P. C.; Raston, C. L.; Skelton, B. W.; White, A. H. *Aust. J. Chem.* **1986**, *39*, 1337.

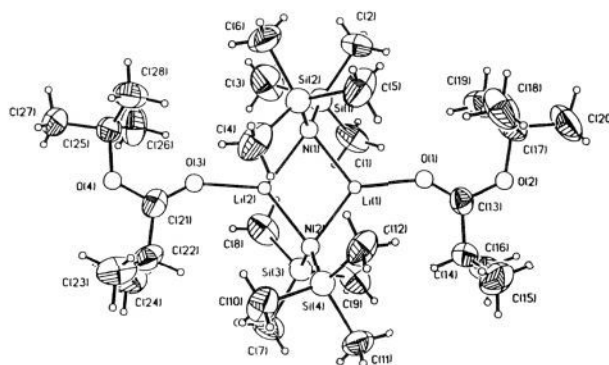
(7) The planes (P1) also bisect both **2a** and **2b** into two crystallographically identical halves.

(8) In the spherical polar coordinate system for determining the directional preferences of ether binding defined by Chakrabarti and Dunitz (Chakrabarti, P.; Dunitz, J. D. *Helv. Chim. Acta* **1982**, *65*, 1482), the relevant ether parameters in **2a** are $d = 1.942 \text{ \AA}$, θ (colatitude) = 90° , and ϕ (longitude) = 180° , and in **2b**, $d = 1.883 \text{ \AA}$, $\theta = 90^\circ$, and $\phi = 180^\circ$.

(9) The size of the cylinders is defined by adjusting the cylinders' radii such that their surface just contacts the van der Waals surface of the TMS groups. The intersection of the cylindrical axes is estimated at $\sim 3.2 \text{ \AA}$ from Li in the plane of the Li–N–Li–N ring.

(10) (a) For theoretical considerations of lithium amide aggregates, see: Sapse, A.-M.; Kaufmann, E.; Schleyer, P. v. R.; Gleiter, R. *Inorg. Chem.* **1984**, *23*, 1569. (b) Romesberg, F. E.; Collum, D. *J. Am. Chem. Soc.*, manuscript in press.

3a LiHMDS / *t*-butyl isobutyrate



3b LiHMDS / *t*-butyl pivalate

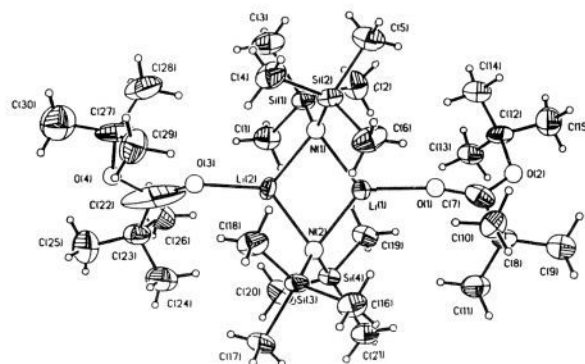


Figure 3. Computer-generated plots with 50% probability ellipsoids of the X-ray crystal structures of the aggregates **3a** and **3b**. The dihedral angle between the plane of the carbonyl group and the Li–N–Li–N core averages $\sim 8^\circ$ in **3a** (Dunitz parameters⁸ $d_{av} = 1.942 \text{ \AA}$, $\theta_{av} = 86.9^\circ$, and $\phi_{av} = 146^\circ$) and $\sim 42^\circ$ in **3b** (Dunitz parameters⁸ $d_{av} = 2.026 \text{ \AA}$, $\theta_{av} = 87.4^\circ$, and $\phi_{av} = 160^\circ$). A complete list of structural parameters is given in the supplementary material.

Thermal ellipsoid plots of these complexes are depicted in Figure 3. In the complex **3a**, the enolizable hydrogen atom points directly toward the basic nitrogen. This configuration is not favorable for enolization since the incipient carbanion cannot be delocalized into the adjacent π orbitals of the carbonyl. Hence the relative stability of the LiHMDS/ester complexes, as exemplified by their characterization by IR, isolation as crystalline solids, and the inability of LiHMDS to enolize α -alkyl-substituted esters, may be attributed to formation of stable, dimeric pre-enolization complexes such as **3a** and **3b** which are sterically incapable of achieving the proper geometry at the α -carbon atom for enolization.

Seebach, Collum, and Boche have already characterized post-enolization reaction complexes in which anionic substrates remain

(11) The LiHMDS/*tert*-butyl isobutyrate aggregate **3a** of molecular composition $(\text{C}_6\text{H}_{16}\text{O}_2)_2 \cdot (\text{C}_6\text{H}_{18}\text{NSi}_2\text{Li})_2$ crystallizes in the monoclinic system, space group P2₁/c with $a = 11.259$ (5) \AA , $b = 35.339$ (6) \AA , $c = 11.375$ (8) \AA , $\beta = 111.08$ (2) $^\circ$ (from 25 orientation reflections, $24^\circ < 2\theta < 26^\circ$), $V = 4223$ (3) \AA^3 , $Z = 4$, $d_{\text{calcd}} = 0.98 \text{ cm}^{-3}$. Intensity data ($\pm h, k, l$); 5814 non-equivalent reflections; $2\theta_{\text{max}} = 45^\circ$) were recorded on a Nicolet R₃m/E diffractometer (Mo K α radiation, $\lambda = 0.71069 \text{ \AA}$; graphite monochromator; $\theta:2\theta$ scans) at approximately -80° C under a stream of nitrogen gas. The crystal structure was solved by direct methods (SHELX-86). Blocked-cascade least-squares refinement (SHELXTL 5.1) of 361 atomic parameters (anisotropic C, N, Si, Li, O; fixed H contributions) converged (maximum shift 0.01 s) at $R = 0.059$ ($R_w = 0.064$, GOF = 1.93) over 4076 reflections with $I > 3.0\sigma(I)$. Crystal data for LiHMDS/*tert*-butyl pivalate (**3b**): $(\text{C}_6\text{H}_{18}\text{NSi}_2\text{Li})_2 \cdot (\text{C}_6\text{H}_{18}\text{NSi}_2\text{Li})_2$; triclinic system; space group, P1; $a = 9.198$ (6) \AA ; $b = 11.291$ (11) \AA ; $c = 22.965$ (13) \AA ; $\alpha = 99.22$ (6) $^\circ$; $\beta = 96.15$ (5) $^\circ$; $\gamma = 110.27$ (6) $^\circ$; $V = 2174$ (3) \AA^3 ; $Z = 2$; $d_{\text{calcd}} = 0.99 \text{ g cm}^{-3}$. Intensity data ($\pm h, \pm k, l$); 6323 non-equivalent reflections ($2\theta_{\text{max}} = 45^\circ$), $R = 0.076$ ($R_w = 0.092$), 379 parameters over 4857 reflections with $I > 3.0\sigma(I)$. Specific details of the diffraction analyses along with tables of atomic coordinates and structural parameters have been submitted as supplementary material and are deposited in the Cambridge Crystallographic Database.

associated with the conjugate acid of the amide base used in their formation.¹² Numerous deuterium-incorporation experiments strongly support the conjecture that such postenolization complexes remain intact in solution. Likewise, we now suggest that the conflicting reports of the ability of LiHMDS to enolize bulky ester and amide substrates are due to the formation of relatively stable preenolization complexes as characterized herein.

Acknowledgment. This work was supported by the National Institutes of Health through Grants GM-35982 and a Research Career Development Award (CA-01330) to P.G.W. The X-ray equipment was purchased with assistance from an instrument grant from the NSF (CHE-8206423).

Supplementary Material Available: Atomic numbering schemes and tables of crystallographic data, atomic positional parameters and thermal parameters, bond lengths and angles, and selected torsion angles for the LiHMDS/*tert*-butyl isobutyrate complex **1a** and the LiHMDS/*tert*-butyl pivalate complex **1b** and IR spectra of **1a**, **1b**, and the LiHMDS/methyl pivalate ester complex (28 pages). Ordering information is given on any current masthead page.

(12) (a) Laube, T.; Dunitz, J. D.; Seebach, D. *Helv. Chim. Acta* **1985**, *68*, 1373. (b) Wanat, R. A.; Collum, D. B.; Van Duyne, G.; Clardy, J.; DePue, R. T. *J. Am. Chem. Soc.* **1986**, *108*, 3415. (c) Buchholz, S.; Harms, K.; Massa, W.; Boche, G. *Angew. Chem., Int. Ed. Engl.* **1989**, *28*(1), 72.

Photochemical Cyclohexane Carbonylation Cocatalyzed by d⁸ Transition Metal Carbonyls and Aromatic Ketones and Aldehydes

William T. Boese and Alan S. Goldman*

Department of Chemistry, Rutgers
The State University of New Jersey
New Brunswick, New Jersey 08903

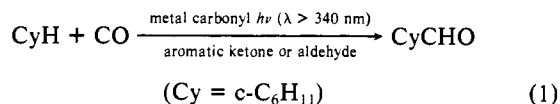
Received June 14, 1991

Revised Manuscript Received October 30, 1991

The catalytic functionalization of alkanes is of great current interest;¹ a potentially important example is carbonylation. Rh(PR₃)₂(CO)Cl (**1**, R = Me) has been found to photochemically catalyze hydrocarbon carbonylation.^{2,3} Recently it was reported that the rate of cyclohexane carbonylation upon irradiation of a 1:1 benzene/cyclohexane solution is 10 times greater than that of a solution of **1** in pure cyclohexane.⁴ This observation was attributed to the inhibition "of secondary photoreactions of cyclohexanecarboxaldehyde including decarbonylation due to the filter effect of benzene".⁴

We find that the *initial* rate of cyclohexane carbonylation ($\lambda > 340$ nm) in a benzene/cyclohexane solution of **1** (7.0 mM) is less than that of a pure cyclohexane solution of **1** ($\phi_{\text{rel}} = 2.9 \times 10^{-5}$).⁵ However, added benzaldehyde (0.10 M) increases the

reaction rate 200-fold ($\phi = 5.8 \times 10^{-3}$, $\phi_{\text{adj}} = 0.20$).⁵ Presumably benzaldehyde produced in the benzene/cyclohexane mixtures is responsible for the increased rate of cyclohexane carbonylation.



Benzophenone, acetophenone, or *p*-(trifluoromethyl)acetophenone have a similar effect on reaction 1. 2-Nonanone and 1-nonanal do not absorb the incident irradiation ($\lambda > 340$ nm) and do not affect the rate. Triphenylene and anthracene absorb 366-nm light and are good triplet sensitizers⁷ like the aromatic carbonyls, but do not accelerate reaction 1. Unlike the aromatic carbonyls, however, their lowest excited states are $\pi-\pi^*$, not $n-\pi^*$, and therefore they do not abstract hydrogen from alkanes, which is a well-known reaction of photoexcited ketones and aldehydes.⁸

The role of the organic carbonyl as the photoactive species in this system is demonstrated by experiments in which the concentration of **1** was varied. An *inverse* dependence of the reaction rate ($\phi_{\text{rel}} = 4.5 \times 10^{-2}$ – 5.4×10^{-3}) on [1] is observed over the range 0.70–7.0 mM **1** as the fraction of light absorbed by (*p*-CF₃C₆H₄)C(O)CH₃ (in competition with **1**) varies in this range from 0.31 to 0.043 ($\phi_{\text{adj}} = 0.12 \pm 0.02$). A similar dependence is observed by varying [Ir(PMe₃)₂(CO)₂Cl] (**2**; vide infra). When [2] is held constant, the rate shows a positive dependence on the concentration of acetophenone over the range 0.0060–0.10 M ($\phi_{\text{rel}} = 1.2 \times 10^{-2}$ – 8.4×10^{-2}) as the fraction of light absorbed by the ketone increases from 0.020 to 0.25. The quantum yield is invariant ($\pm 5\%$) over a 10-fold intensity range (2 mM **2**, 0.10 M acetophenone), arguing against the possibility of a two-photon mechanism.

1-Catalyzed benzene photocarbonylation is not accelerated by aromatic ketones. This selectivity is consistent with a proposed role of the photoexcited ketone as a hydrogen-abstraction agent since the aryl–hydrogen bond is too strong for the hydrogen to undergo abstraction. The presence of a good hydrogen donor, PhCHMeOH (1.0 M), reduces the rate of reaction 1 by 40% (2 mM **2**, 0.10 M acetophenone). Irradiation of a 1:1 C₆H₁₂/C₆D₁₂ solution of **2** (4.0 mM) and Ph₂CO (0.033 M) yields the following ratio of isotopomers: C₆H₁₁CHO:C₆H₁₁CDO:C₆D₁₁CHO:C₆D₁₁CDO = 70.9:12.2:14.8:2.1. The isotope effect, $k_{\text{H}}/k_{\text{D}} = 4.9$, is consistent with known isotope effects for H abstraction by photoexcited ketones⁹ and contrasts with $k_{\text{H}}/k_{\text{D}} = 1.1$ for **1**-photocatalyzed benzene carbonylation.

Presuming the photoexcited ketone to cleave the alkane C–H bond, we considered that metal carbonyls other than **1** might also be effective cocatalysts. Indeed, the following metal carbonyls with d⁸ electronic configurations are all effective (0.10 M PhC(O)Me): RhL₂(CO)Cl (L = PPh₃, P^tPr₃), Ru(CO)₃(dmpe), and **2**.¹⁰ In the absence of ketone, none of these complexes significantly catalyze cyclohexane carbonylation.^{11,12}

(5) All photochemical experiments (cyclohexane solvent) were performed as described previously.⁶ Relative quantum yields, ϕ_{rel} , were obtained based on rates relative to a carbonylation reaction for which the absolute ϕ was measured (0.22 mM h⁻¹ CyCHO, 7 mM **1**, 0.10 M PhC(O)Me, $\lambda = 366$ nm, $I = 1.4 \times 10^{-7}$ einstein/s, 2.0 mL, $\phi = 1.0 \times 10^{-3}$). Use of a Corning CS-0-52 cutoff filter ($\lambda > 345$ nm) instead of a "monochromatic" (366 nm) filter combination (Corning CS-0-52 and Corning CS-7-60) yielded a rate of 0.62 mM/h. Thus $\phi_{\text{rel}} = \{([d[\text{CyCHO}]/dt]/(0.62 \text{ mM h}^{-1})) \times 1.0 \times 10^{-3}\}$ (see supplementary material for experimental details). ϕ_{adj} is defined as moles of product per einstein absorbed by the ketone or aldehyde, i.e., $\phi_{\text{adj}} = \phi_{\text{rel}} \times \{([\text{ketone}] \epsilon_{\text{ketone}} + [\text{M-CO}] \epsilon_{\text{M-CO}})/[\text{ketone}] \epsilon_{\text{ketone}}\}$.

(6) Maguire, J. A.; Boese, W. T.; Goldman, A. S. *J. Am. Chem. Soc.* **1989**, *111*, 7088.

(7) Herkstroeter, W. G.; Lamola, A. A.; Hammond, G. S. *J. Am. Chem. Soc.* **1964**, *86*, 4537.

(8) Turro, N. J. *Modern Molecular Photochemistry*; Benjamin Cummings: Menlo Park, CA, 1978; pp 362–368.

(9) Reference 8, p 385.

(10) Cyclohexane photocarbonylation occurs to a slight extent in solutions of aromatic ketones in the absence of metal carbonyl under 800 Torr of CO ($\lambda = 366$ nm, 0.10 M (*p*-CF₃C₆H₄)C(O)CH₃, $\phi_{\text{rel}} = \phi_{\text{adj}} = 0.0028$). Yields are significantly higher under higher pressures: e.g., 400 psi of CO, $\phi_{\text{rel}} = \phi_{\text{adj}} = 0.077$). Boese, W. T.; Goldman, A. S., to be published.

(1) For reviews in the area of C–H bond activation by homogeneous transition-metal systems, see: (a) Bergman, R. G. *Science (Washington, D.C.)* **1984**, *223*, 902. (b) Crabtree, R. H. *Chem. Rev.* **1985**, *85*, 245. (c) Halpern, J. *Inorg. Chim. Acta* **1985**, *100*, 41. (d) Jones, W. D.; Feher, F. J. *Acc. Chem. Res.* **1989**, *22*, 91. (e) *Activation and Functionalization of Alkanes*; Hill, C., Ed.; John Wiley and Sons: New York, 1989 and references therein.

(2) (a) Fisher, B. J.; Eisenberg, R. *Organometallics* **1983**, *2*, 764–767. (b) Kunin, A. J.; Eisenberg, R. *J. Am. Chem. Soc.* **1986**, *108*, 535–536. (c) Kunin, A. J.; Eisenberg, R. *Organometallics* **1988**, *7*, 2124–2129. (d) Gordon, E. M.; Eisenberg, R. *J. Mol. Catal.* **1988**, *45*, 57–71.

(3) (a) Sakakura, T.; Tanaka, M. *J. Chem. Soc., Chem. Commun.* **1987**, 758–759. (b) Sakakura, T.; Tanaka, M. *Chem. Lett.* **1987**, 249–254. (c) Sakakura, T.; Tanaka, M. *Chem. Lett.* **1987**, 1113–1116. (d) Sakakura, T.; Sasaki, K.; Tokunaga, Y.; Wada, K.; Tanaka, M. *Chem. Lett.* **1988**, 155–158.

(4) Sakakura, T.; Sodeyama, T.; Sasaki, K.; Wada, K.; Tanaka, M. *J. Am. Chem. Soc.* **1990**, *112*, 7221–7229.